ISSN 1674-1056
http://cpb.iphy.ac.cn
http://iopscience.iop.org/cpb
中国物理 B
Chinese Physics
中国物理
Chinese Physics B

Role of the dressed and bound states on below-threshold harmonic generation of He atom

Jian-Wei Zhou(周建伟), Zhi-Hong Jiao(焦志宏), Peng-Cheng Li(李鹏程), Xiao-Xin Zhou(周效信)
Citation: Chin. Phys. B . 2019, 28(10): 103202 . **doi:** 10.1088/1674-1056/ab3bd4
Journal homepage: http://cpb.iphy.ac.cn; http://iopscience.iop.org/cpb

What follows is a list of articles you may be interested in

Trajectory analysis of few-cycle strong field ionization in two-color circularly polarized fields

Yan Huang(黄燕), Chaochao Qin(秦朝朝), Yizhu Zhang(张逸竹), Xincheng Wang(王新成), Tian-Min Yan(阎天民), Yuhai Jiang(江玉海)
Chin. Phys. B . 2019, 28(9): 093202 . **doi:** 10.1088/1674-1056/ab3444

Coherent control of fragmentation of methyl iodide by shaped femtosecond pulse train

Qiu-Nan Tong(佟秋男), De-Hou Fei(费德厚), Zhen-Zhong Lian(廉振中), Hong-Xia Qi(齐洪霞), Sheng-Peng Zhou(周胜鹏), Si-Zuo Luo(罗嗣佐), Zhou Chen(陈洲), Zhan Hu(胡湛)
Chin. Phys. B . 2019, 28(9): 093201 . **doi:** 10.1088/1674-1056/ab33f3

Controlling Rydberg excitation process with shaped intense ultrashort laser pulses

Xiao-Yun Zhao(赵晓云), Chun-Cheng Wang(王春成), Shi-Lin Hu(胡师林), Wei-Dong Li(李卫东), Jing Chen(陈京), Xiao-Lei Hao(郝小雷)
Chin. Phys. B . 2019, 28(8): 083202 . **doi:** 10.1088/1674-1056/28/8/083202

Dependence of photoelectron-momentum distribution of H_2^+ molecule on orientation angle and laser ellipticity

Hong-Dan Zhang(张宏丹), Si-Qi Zhang(张思琪), Lei Ji(纪磊), Qi Zhen(甄琪), Jing Guo(郭静), Xue-Shen Liu(刘学深)
Chin. Phys. B . 2019, 28(5): 053201 . **doi:** 10.1088/1674-1056/28/5/053201

The ac Stark shifts of the terahertz clock transitions of barium

Yu Geng-Hua, Geng Ying-Ge, Li Long, Zhou Chao, Duan Cheng-Bo, Chai Rui-Peng, Yang Yong-Ming
Chin. Phys. B . 2015, 24(10): 103201 . **doi:** 10.1088/1674-1056/24/10/103201

SPECIAL TOPIC — Strong-field atomic and molecular physics

Role of the dressed and bound states on below-threshold harmonic generation of He atom*

Jian-Wei Zhou(周建伟), Zhi-Hong Jiao(焦志宏)†, Peng-Cheng Li(李鹏程)‡, and Xiao-Xin Zhou(周效信)§

Key Laboratory of Atomic and Molecular Physics and Functional Materials of Gansu Province, College of Physics and Electronic Engineering, Northwest Normal University, Lanzhou 730070, *China*

(Received 11 May 2019; revised manuscript received 5 July 2019; published online 17 September 2019)

High-order harmonic generation below ionization threshold of He atom in the laser field is investigated by solving the three-dimensional time-dependent Schrödinger equation. An angular momentum-dependent model potential of He atom was used for getting the accurate energy levels of singlet states. The satellite-peak structures of the below-threshold harmonic generation (BTHG) of He are observed. We analyze the emission properties of the BTHG by employing a synchrosqueezing transform technique. We find that the satellite-peak structures have two types related to two kinds of transitions. One is the transition of the dressed states of the excited states, the other is the transition between the excited states and the ground state in the field-free case. Furthermore, our results show that the maximum Stark shift of the 2p state is about $0.9U_p$ (penderomotive energy), and that of the 4p state is about $1.0U_p$. It indicates that the energy difference between some satellite- and main-peaks of the BTHG can be used to measure the maximum Stark shift of the excited states of He atom in the laser field.

Keywords: harmonic generation below threshould ionization, dress state, Stark shift

PACS: 32.80.Rm, 42.65.Ky, 42.65.Re **DOI:** 10.1088/1674-1056/ab3bd4

1. Introduction

High-order harmonic generation (HHG) radiated from atoms or molecule in intense laser field has attracted considerable attention during the past decades. Based on their potential applications, such as attosecond time-resolved spectroscopy,[1,2] observation and control of the electronic dynamical processes in attosecond timescale,[3–6] researchers pay a close attention to the HHG at the plateau and near the cutoff region because its important application in ultra-short attosecond pulse. The generated high-energy photons can be well explained by the semiclassical three-step model.[7] First, the electron in atoms is ionized by the tunneling, then it propagates in the laser field and is driven back towards the parent ions (rescattering) and gains energy. Finally, the electron recombines into the ground state and emits the photons to produce the high-order harmonics. The maximum harmonic photon energy is located approximately at the cutoff energy $I_p + 3.17U_p$, where I_p is the atomic ionization potential and U_p is the ponderomotive potential of electron in the laser field. Recently, some researchers[8,9] focus on high-order harmonic generation below ionization threshold of atoms because its applications in a high-repetition-rate and high-intensity light source.[10] However, the below-threshold harmonic generation (BTHG) process cannot be explained by the three-step model, because the BTHG radiation involves the transition between the bound states of atom beside the electron rescattering by the parents ions, so both the continuum states and the bound states of the target atom play an important role in the production of HHG radiation, and the HHG emission process become more complex. Li *et. al.*[11] have studied the dynamical origin of HHG below ionization threshold of Cs atom. Camp *et. al.*[12] have studied the HHG enhancement below and near the ionization threshold of He in the laser field with a 400-nm-wavelength above. They found that the enhancement of HHG contributes to multiphoton resonance between the ground state and the stark excited state. Beaulieu *et. al.*[13] have investigated the structure of HHG spectra produced near the ionization threshold of Ar atoms. They observed both the usual odd harmonic peaks and the satellite-peaks structure of Ar atom. They also confirmed that the excited states of atom play an important role in the production of the satellite- peaks of HHG. Yan *et al.* have studied the BTHG from hydrogen atom in the laser pulse.[14] Xiong *et al.*[15] have observed the new below-threshold harmonics when the electron from hydrogen atom was ionized from the excited states and recombined to the ground state. For the molecules, Avanaki *et al.*[16] found that the 3rd, 5th, and 7th harmonics of H_2^+ molecular ion were split in double peaks due to the resonance between

*Project supported by the National Natural Science Foundation of China (Grant Nos. 11674268, 11764038, and 11765018) and the Scientific Research Foundation of Physics of CPEE–NWNU and NWNU-LKQN-17-1, China.

†Corresponding author. E-mail: jiaozh@nwnu.edu.cn

‡Corresponding author. E-mail: lipc@nwnu.edu.cn

§Corresponding author. E-mail: zhouxx@nwnu.edu.cn

© 2019 Chinese Physical Society and IOP Publishing Ltd

the ground $1\sigma_g$ and the first excited $1\sigma_u$ states, and we[17] explain the reason due to the interference of the different cycles between the lowest two bound states of H_2^+ ion by using a two-state model.[18] Therefore, the bound states have an important role on the BTHG of atom and molecule.

In this paper, we focus on the BTHG below the ionization threshold of He atom. We calculate the BTHG spectra of He atom by solving the three-dimensional time-dependent Schrödinger equation (TDSE) of He atom with the angular momentum model potential for the accurate bound states structures of the singlet state. We find not only the traditional odd peaks but also the satellite-peaks of the BTHG of He atom, and the origin of the satellite-peaks is explored by means of the time-frequency transform and the energy relation of the transitions.

2. Theoretical method

The BTHG of helium atom in the laser field can be obtained by solving the TDSE of He atom with a single-electron approximation. In the length gauge, the TDSE of He atom in dipole approximation can be written as (atomic units are used, unless otherwise stated)

$$\mathrm{i}\frac{\partial}{\partial t}\psi(\boldsymbol{r},t)=\hat{H}\psi(\boldsymbol{r},t)=[H_0(\boldsymbol{r})+\hat{V}(\boldsymbol{r},t)]\psi(\boldsymbol{r},t), \quad (1)$$

where H_0 is the field-free Hamiltonian of a He atom:

$$H_0=-\frac{1}{2}\nabla^2+\sum_l|\mathrm{Y}_l^0\rangle V_l\langle\mathrm{Y}_l^0|, \quad (2)$$

here, Y_l^0 is the spherical harmonic function, V_l is the angular momentum-dependent model potential of He atom[19]

$$V_l=-\frac{\alpha}{2r^4}\mathrm{W}_6\left(\frac{r}{r_c}\right)-\frac{1}{r}-\left(\frac{N-S}{r}+A_1\right)\mathrm{e}^{-\mathrm{B}_1 r}-\left(\frac{S}{r}+A_2\right)\mathrm{e}^{-\mathrm{B}_2 r}, \quad (3)$$

where α is the dipole polarization rate of He^+ ion, r_c, A_1, A_2, B_1, and B_2 can be found in Ref. [20], $W_n(x)$ is a truncation function, which can be expressed as:

$$W_n(x)=1-\left[1+x+\frac{(2x)^2}{2!}+\cdots+\frac{(nx)^n}{n!}\right]\mathrm{e}^{-nx}, \quad (4)$$

$V(\boldsymbol{r},t)$ is the interaction between He atom and laser field, which can be written as

$$\hat{V}(\boldsymbol{r},t)=-\boldsymbol{E}(t)\cdot\boldsymbol{r}=-E_0 z f(t)\sin\omega t, \quad (5)$$

where E_0, ω, $f(t)$ are the electric field amplitude, the angular frequency, and the envelope of the laser pulse, respectively.

The time-dependent generalized pseudo-spectral (short as TDGPS) method[21] is used to solve the TDSE (1) in spherical coordinates accurately. This method takes the non-uniform optimal spatial discretization of the coordinates. The time propagation of the wave function under this method is performed by the split operator method as follows:

$$\psi(\boldsymbol{r},t+\Delta t)=\exp\left(-\mathrm{i}\hat{H}_0\frac{\Delta t}{2}\right)\times\exp\left[-\mathrm{i}\hat{V}\left(r,\theta,\frac{t+\Delta t}{2}\right)\Delta t\right]\times\exp\left(-\mathrm{i}\hat{H}_0\frac{\Delta t}{2}\right)\psi(\boldsymbol{r},t)+O(\Delta t^3). \quad (6)$$

Once obtaining the time-dependent wave function of the interaction between atom and laser field, we can calculate the expectation value of the induced dipole moment in the length form:

$$d_{\mathrm{L}}(t)=\langle\psi(\boldsymbol{r},t)|z|\psi(\boldsymbol{r},t)\rangle. \quad (7)$$

The HHG power spectra in the length form can be obtained using the Fourier transformation of the time-dependent dipole moment $d_{\mathrm{L}}(t)$:

$$p_{\mathrm{L}}(\omega)=\left|\frac{1}{t_{\mathrm{i}}-t_{\mathrm{f}}}\int_{t_{\mathrm{i}}}^{t_{\mathrm{f}}}d_{\mathrm{L}}(t)\,\mathrm{e}^{\mathrm{i}\omega t}\mathrm{d}t\right|^2. \quad (8)$$

To understand the dynamic process of the HHG, we perform the time-frequency analysis by means of the synchrosqueezing transform (SST).[11] Compared with traditional TF techniques, such as Gabor transform, Morlet transform, *etc*., the SST can resolve the intrinsic blurring in the TF spectra below the ionization threshold and produce a clear spectrum.

3. Results and analysis

By using the method mentioned above, we have calculated the BTHG of He atom in the laser field when the initial state of the atom is in the ground state. In our calculation, we choose a laser electric field with a 34-cycles and $\sin^2$ envelope. In Fig. 1, we show the calculated BTHG of He atom for the driving wavelength 335 nm at the intensities $I=1.0\times10^{14}$ W/cm^2, $I=1.5\times10^{14}$ W/cm^2, and $I=2.0\times10^{14}$ W/cm^2, and for the driving wavelength 200 nm, 335 nm, and 470 nm in the driving intensity $I=2.0\times10^{14}$ W/cm^2, respectively.

In Fig. 1(a), the unusual harmonic peaks (satellite-peaks) appear at the left side of the normal 3rd order to the 9th order, and the peaks become stronger and have a shift with the laser intensities, and the peaks disappear at 200-nm and 470-nm wavelengths [see Fig. 1(b)]. The results for He atom are similar to that of hydrogen atom in Ref. [15]. The satellite-peaks for hydrogen atom are attributed to the transition between the pre-excited bound states to ground state.[15] They identified the satellite-peaks of the 5th and 7th orders as the 2p–1s and 3p–1s transitions, respectively. However, the satellite-peaks of the 5th (or 3rd) order of He atom cannot produce from the transition between the excited states and the ground state because the energy level differences between the excited states

to the ground state, which is larger than the energy location of the peak, even between the first excited state and the ground state. In order to confirm the origin of the satellite-peaks of the BTHG, we perform the time-frequency (TF) analysis by means of SST method for the BTHG at driving intensity $I = 2.0 \times 10^{14}$ W/cm^2 with a 335-nm wavelength, as shown in Fig. 2. The satellite-peaks of the 3rd, 5th, and 9th orders are mainly emitted on the falling edge of the laser pulse as shown in Fig. 2(a). This is consistent with the e-HHG results reported in Ref. [13]. Namely, the e-HHG attributed to the ionization of the pre-excited states, then recombination to the ground state of Ar atom. However, here the emission characteristics of the satellite-peaks of the 3rd, 5th, and 9th orders of He atom are different from that of Ar atom because the energy locations of the satellite-peaks for He atom are lower than the transition energy. In the case of He atom, the satellite-peaks of the 3rd, 5th, and 9th orders emit only in the falling edge of the laser pulse, while the satellite-peaks of the 7th order does not only emit on the falling edge, but also after the laser end. This indicates that the side peak of the 7th order emission differs from the other peaks. The fact that the emission occurs after the laser suggest a part of the satellite-peaks of the 7th order coming from the transition between the field-free excited state to the ground state. Because the life of the atomic excited state is nanosecond scale in general, and the width of laser pulse is in femtosecond level, therefore, in the excited-state atom after laser propagation, within the scope of the nanosecond order of magnitude, there is still a radiation. We can identify it belong which the transition based on the position of the satellite-peaks. The lowest excited state for the allowed transition to the ground state of He atom is 2p, $\Delta E_{2p,1s} = E_{2p} - E_{1s} = 0.78$ a.u., a photon energy for 335 nm is 0.136 a.u., $\Delta E_{2p,1s} = 5.7\omega$. Obviously, the satellite-peaks corresponding to transition from 2p state to the ground state should be near the 6th order, but satellite-peaks of emission appear at 6.1 and 6.4 orders at the end of the laser field.

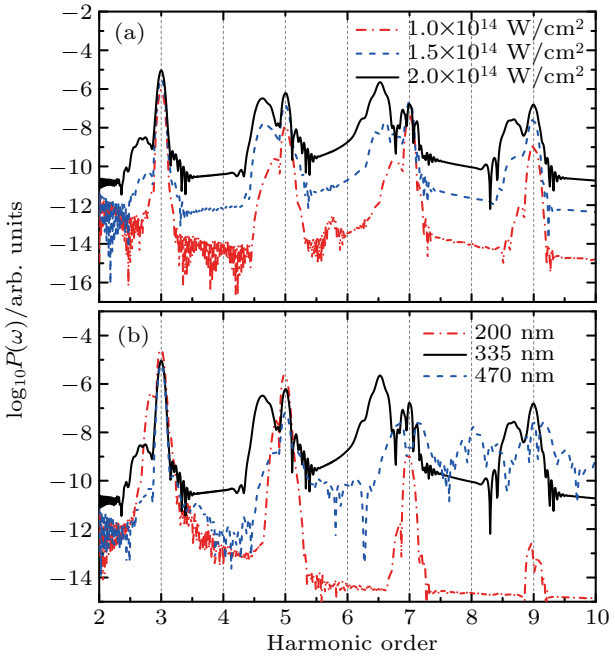


Fig. 1. The BTHG spectra of He atom driven by the laser pulses with different intensities (a) and wavelengths (b).

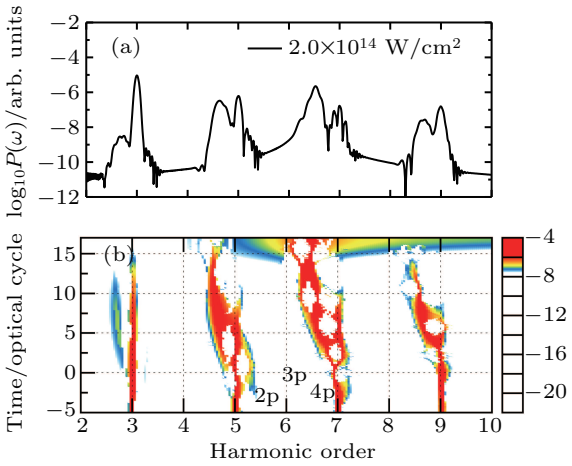


Fig. 2. The BTHG spectra (a) of He in the laser pulse with wavelength 335 nm and SST (b) analysis.

Next, we will recognize the contributions of excited states to the satellite-peaks of left-side of the 7th order near the end of the laser field. In Fig. 2(b), at the end of the laser pulse, the satellite-peaks near the 7th order locates at 6.1ω and 6.4ω. For the transition between 4p, 3p, and 1s states, the energy differences $\Delta E_{4p,1s}$, $\Delta E_{3p,1s}$ are 6.4ω and 6.3ω, respectively. Therefore, we speculate that the 4p and 3p states have a certain number of populations when the laser pulse is over, which leads to the emission caused by the transition from 4p (3p) to 1s state. To confirm this result, we can project the time-dependent wave function on the 4p, 3p, and 2p states during near the end of the falling edge of the laser pulse. We find that the population of 4p and 3p state is larger than 2p state case, as shown in Fig. 6(a). As the analysis above, the satellite-peaks of the 7th order in Fig. 2(b) are composed of two parts. One part can be attributed to the transition between the 4p, 3p, and 1s states in the field free, and the other part comes from the transient Stark shift of the 4p, 3p states in the laser field. The satellite-peaks of the 3rd, 5th, and 9th orders are only generated by the transition between the dressed states. Furthermore, we find that the difference between the peak position of these satellite-peaks is approximately 2ω. This indicates that the satellite- peaks of the new set of harmonics have a energy relationship with new energy levels. To explain this, we consider the energy relation of the BTHG to the atomic dress states in the laser field. We defined that the transient Stark shift of the bound state is U_x at time t, the emission energy of the satellite-peaks for the BTHG can be given by

$$(E_{jp} \pm m\omega + U_x) - (E_{1s} \pm n\omega) = q\hbar\omega, \tag{9}$$

where $E_{jp} \pm m\omega$, and $E_{1s} \pm n\omega$ are the energy levels of the zero order dress states of the excited state jp, and the ground state 1s of atom in the laser field, respectively,[22] q is a non-integer, $q\hbar\omega$ is the energy of a photon in the satellite-peaks. The energy levels for the dress states of 3p and 1s of He are shown in Fig. 3. From the result shown, we can easily explain the reason that the interval between the adjacent satellite-peaks is 2ω.

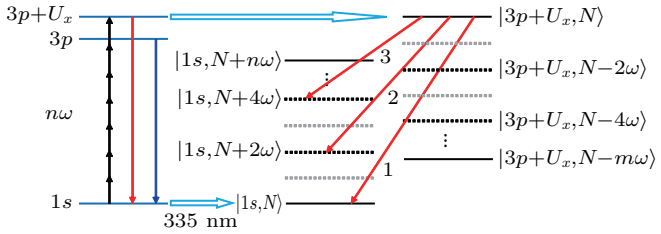


Fig. 3. The zero-order dressed states from 1s and 3p states for He atom in laser field.

According to multi-photon process, the BTHG is the result of the transition between the dressed states formed by the same state in field-free (not shown in Fig. 3). Here, we can understand for the satellite-peaks of the BTHG as the transition between the dressed states formed by some different states with field-free. The corresponding transitions for the satellite-peaks are shown schematically in Fig. 3. For example, the transition 1 in the figure corresponds to the satellite-peaks of the 7th order, the transition 2 emits the satellite-peaks of the 5th order, and the transition 3 gives the satellite-peaks of the 3rd, even it is weak. We find that the adjacent interval of the satellite-peaks is 2ω. Figure 3 shows an instantaneous transition diagram for the satellite-peaks. In fact, the radiation energy will change with time propagation, but the energy difference of the radiation at any time is always 2ω, as shown in Fig. 2 (also seen in Fig. 4). Because the transition for the satellite-peaks shown in Fig. 2 involves the dressed states of 3p, 4p states, the shape of the SST figure is complex. If only a single excited state is involved, we can use the SST diagram to calculate the instantaneous stark shift U_x of the atomic excited state at a given time, $U_x(t) = [E_0 f(t)]^2/4\omega^2$ called the instantaneous stark shift of the excited state.

To study the characteristics of the satellite-peaks of the BTHG when only one excited state has a distinct population, for example, 2p state, we calculated the low-order harmonics of He atom driven by a laser pulse with the wavelength 470 nm and intensity $I = 1.4 \times 10^{14}$ W/cm^2, and the corresponding time-frequency analysis (SST). Our results are shown in Fig. 4. we can see that only the satellite-peaks near the 8th order emits at the end of laser pulse, which indicates that the emission is due to the result of the transition between the excited state and the ground state in field-free. Next, we will analyze this process according to Eq. (9) combined with Fig. 4(b). We can estimate the instantaneous Stark shift value if any harmonic energy of the satellite-peaks at any time is chosen. For example, if $q\hbar\omega = 8.5\omega$, then according to Eq. (9), we can get $U_x = 0.45\omega$, the corresponding transition is the process 1 in Fig. 3 (but 3p is replaced by 2p in the figure). If $q\hbar\omega = 9\omega$, due to $\Delta E_{2p,1s} = 0.78$ a.u. according to Eq. (9), then $U_x = 0.09$ a.u., which is very close to U_p (U_p is ponderomotive energy, here $U_p = 0.1$ a.u.). That explains very well the reason that the energy difference between the satellite-peaks and the 9th order is $0.9U_p$. It also suggests that the biggest Stark shift for the 2p state of He atom in laser field just is the difference, *i.e.*, $0.9U_p$.

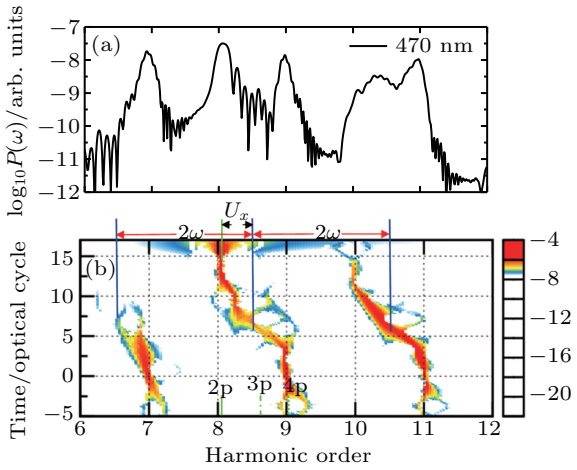


Fig. 4. The BTHG spectra (a) of He in laser pulse with wavelength 470 nm, intensity 1.4×10^{14} W/cm^2, and SST (b) analysis.

For the satellite-peaks of the 7th order, although the side peak does not appear in Fig. 4(a), there is a red shift for the order, which is the combined contribution of the normal HHG and transition of the dressed states shown in SST analysis (Fig. 4(b)). For the side peak of the 11th order, it can be understood as the transition from $|2p + U_x, N + 2\omega\rangle$ to $|1s, N\rangle$ in Fig. 3 (note: 3p is replaced by 2p in the figure). That is the reason for the interval of the satellite-peaks is 2ω.

If we choose the laser wavelength is 425 nm, intensity is 1.4×10^{14} W/cm^2, we calculated the BTHG of He atom. The results are shown in Fig. 5. From the figure, we can find some satellite-peaks still appear. In the SST analysis, a satellite-peaks of the 9th order is still emission even at the end of the laser pulse, and the main contribution of the satellite-peaks comes from the emission. We can calculate $\Delta E_{4p,1s} = 8.16\omega$, so the emission should be the transition from the 4p excited state to the ground state in field-free, which means a certain number of population in 4p state at the end of laser pulse. Based on the difference between the satellite-peaks and main peak of the 9th order, we can estimate the difference is $0.8\omega = 0.086$ a.u., and by calculating the $U_p = E_0^2/4\omega^2 = 0.087$ a.u. both results are almost the same, which indicates the maximum Stark shift of the excited state 4p of He atom in laser field is $1.0U_p$, *i.e.*, the energy difference between the side peak and the main peak of the 9th order just is the maximum Stark shift.

It should be pointed out that the position of the satellite-peaks of the BTHG would change with the laser intensity when the satellite-peak emission only comes from the transition between the dressed states in laser field. And when the satellite-peak emission originated from two kinds of transition, *i.e.*, the transition between the dressed states in laser field and the excited state to ground state in field-free, for the part of the transition between the excited state to ground states in the field-free, the position of the satellite-peaks is independent of the laser intensity. If the contribution of the transition between the dressed states is dominant, the position of the satellite-peak will still change with the laser intensity (as shown in Fig. 1(a)). Hence, when the contribution of the satellite-peaks of BTGH from the excited state to ground state in field-free is dominant, the energy difference between the satellite-peak and the main peak can be used to determine the Stark shift of the excited state of He atom.

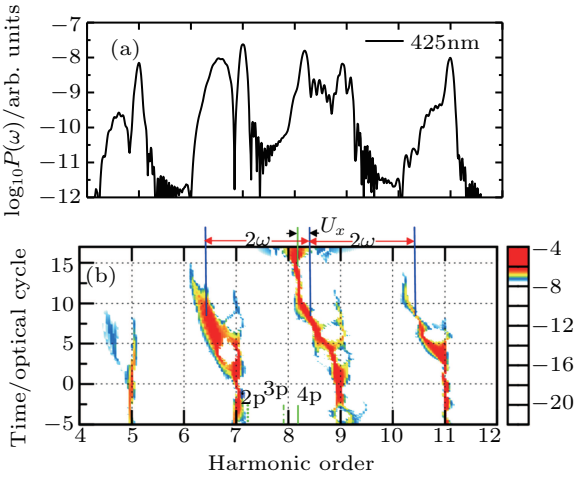


Fig. 5. The BTHG spectra (a) of He in laser pulse with wavelength 425 nm, intensity 1.4×10^{14} W/cm^2, and SST (b) analysis.

For the analysis of the side peaks above is based on the energy relation of atomic energy levels and Stark shift, which include the transition of 4p–1s or 3p-1s (Fig. 2) and 2p–1s (Fig. 4). We can also confirm the transitions near the end of laser pulse mentioned above occur by the electron population in 2p, 3p, and 4p states of He atom driven by the laser intensity 2.0×10^{14} W/cm^2 with wavelength 335 nm, and intensity 1.4×10^{14} W/cm^2 with wavelength 470 nm and 425 nm, respectively. The results are shown in Fig. 6.

In the first case (Fig. 6(a)), the populations on the excited states 4p and 3p are much higher than that of 2p state after the 16th cycle. The population of 2p state is almost zero after 17 cycles, and the population on 4p state is higher than 3p. Therefore, that is the reason that emission probability for 4p–1s transition is much stronger than that of 3p–1s transition at the end of the laser in the time-frequency analysis diagram of Fig. 2; In the second case (Fig. 6(b)), the population of 2p state is a significantly higher than that of 3p and 4p, so emission line for the transition of 2p–1s is signification high near the laser over; For the third case (Fig. 6(c)), only the population of 4p is high, therefore, the side peak radiation involving 4p–1s is strong, which is consistent with the results given in the corresponding SST figures.

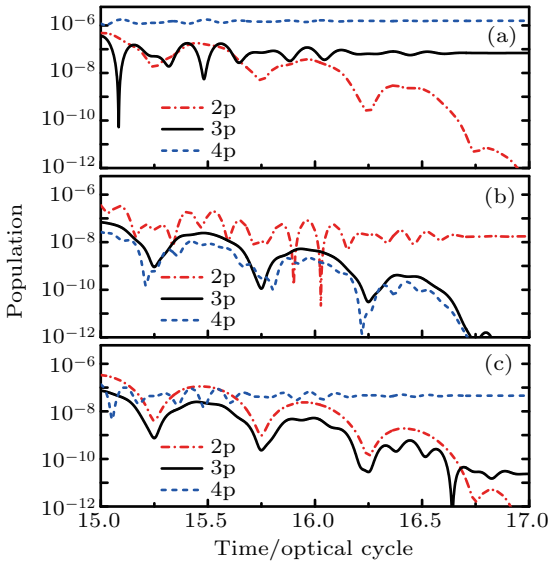


Fig. 6. The population of the excited states 2p, 3p, and 4p of He near the end of laser pulse for (a) $I=2.0\times10^{14}$ W/cm^2, $\lambda=335$ nm; (b) $I=1.4\times10^{14}$ W/cm^2, $\lambda=470$ nm; and (c) $I=1.4\times10^{14}$ W/cm^2, $\lambda=425$ nm.

4. Conclusions

We have investigated the BTHG emission of He atom driven by a laser pulse by solving 3D TDSE. In our study, we use the precise model potential of He atom, which can give the accurate singlet state energy levels. Meanwhile, we use the SST method to analyze the emission process of the BTHG in detail because the method has a high resolution for energy. In our study, we found the satellite-peaks of the BTHG for He atom appear. Through the analysis of SST, we are able to identify the contribution of some satellite-peaks only comes from the dressed states in laser field, and some peaks caused by the transition of the excited state to the ground state in field-free and of the dressed states in the laser field. For the former, we can explain the reason that the interval between the adjacent satellite-peaks is 2ω because the transition takes place in the dressed states formed from the different states in field-free. For the later, if only one excited state has high population, then the energy difference between the satellite-peaks and the main peak means the largest Stark shift for the excited state in laser field. Based on the structure of the satellite-peaks, we can obtain that the maximum Stark shift of 2p state for helium atom in the laser field is $0.9U_p$, and that for the 4p excited state is about $1.0U_p$.

References

[1] Hentschel M, Kienberger R, Spielmann Ch, Reider G A, Milosevic N, Brabec T, Corkum P, Heinzmann U, Drescher M and Krausz F 2001 *Nature* **414** 509

[2] Drescher M, Hentschel M, Kienberger R, Tempea G, Spielmann C, Reider G A, Corkum P B and Krausz F 2001 *Science* **291** 1923
[3] Chini M, Zhao K and Chang Z 2014 *Nat. Photon.* **8** 178
[4] Silva F, Teichmann S M, Cousin S L, Hemmer M and Biegert J 2015 *Nat. Commun.* **6** 6611
[5] Henkel J, Witting T, Fabris D, Lein M, Knight P L, Tisch J W G and Marangos J P 2013 *Phys. Rev. A* **87** 043818
[6] Bian X B and Bandrauk A D 2012 *Phys. Rev. Lett.* **108** 263003
[7] Corkum P B 1993 *Phys. Rev. Lett.* **71** 1994
[8] Spott A, Becker A and Jaron-Becker A 2015 *Phys. Rev. A* **91** 023402
[9] Xiong W H, Geng J W, Tang J Y, Peng L Y and Gong Q 2014 *Phys. Rev. Lett.* **112** 233001
[10] Cingoz A, Yost D C, Allison T K, Ruehl A, Fermann M E, HartlI and Ye J 2012 *Nature* **482** 68
[11] Li P C, Sheu Y L, Laughlin C and Chu S I 2015 *Nat. Commun.* **6** 7178
[12] Camp S, Schafer K J and Gaarde M B 2015 *Phys. Rev. A* **92** 013404
[13] Beaulieu S, Camp S, Descamps D, *et al.* 2016 *Phys. Rev. Lett.* **117** 203001
[14] Yan Y, Guo F M, Wang J, Chen J G and Yang Y J 2018 *Chin. Phys. B* **27** 083202
[15] Xiong W H, Jin J Z, Peng L Y and Gong Q H 2017 *Phys. Rev. A* **96** 023418
[16] Avanaki K N, Telnov D A, Jooya H Z and Chu S I 2015 *Phys. Rev. A* **92** 063811
[17] Du L L, Wang G L, Li P C, Zhou X X and Zhao Z X 2018 *Phys. Rev. A* **97** 023404
[18] Du L L, Wang G L, Li P C and Zhou X X 2018 *Chin. Phys. B* **27** 113201
[19] Chu X, Chu S I and Laughlin C 2001 *Phys. Rev. A* **64** 013406
[20] Li P C, Laughlin C and Chu S I 2014 *Phys. Rev. A* **89** 023431
[21] Tong X M and Chu S I 1997 *Chem. Phys.* **217** 119
[22] Cohen-Tannoudji C, Dupont-Roc and Grynberg G 1992 *Atom-Photon Interaction, Basic Processes and Applications* (John Wiley & Sons, Inc.)